Limnol. Oceanogr., 49(6), 2004, 2046–2057

Pathways of organic carbon oxidation in a deep lacustrine sediment, Lake Michigan

Uffe Thomsen
Danish Technological Institute, Chemistry and Water Technology, DK-8000 Aarhus C, Denmark

Bo Thamdrup[1]
Danish Center for Earth System Science, Institute of Biology, University of Southern Denmark, DK-5230 Odense M, Denmark

David A. Stahl
Civil and Environmental Engineering, 302 More Hall, Box 352700, University of Washington, Seattle, Washington 98195-2700

Donald E. Canfield
Danish Center for Earth System Science, Institute of Biology, University of Southern Denmark, DK-5230 Odense M, Denmark

Abstract

Rates of microbial iron reduction and other pathways of organic carbon (C_{org}) oxidation were investigated in sediment from a 100-m deep site in Lake Michigan. Total benthic mineralization rates of 6.8 and 8.0 mmol m^{-2} d^{-1}, respectively, were determined from benthic flux measurements and by summation of dissolved inorganic carbon (ΣCO_2) accumulation rates measured in anoxic incubations of sediment in discrete depth intervals to 18 cm depth. Carbon oxidation rates were highest near the sediment surface and decreased asymptotically toward zero. A C_{org} half-life of 0.06 yr was estimated in the oxic zone, but the half-life increased by more than two orders of magnitude in the deep anoxic layers. Mineralization in the oxic zone (0–2.1 cm) accounted for 37% of the total ΣCO_2 production, whereas microbial iron reduction was the most important pathway of carbon oxidation, accounting for 44%; sulfate reduction accounted for 19%, and methanogenesis was negligible. Denitrification accounted for <3% of C_{org} oxidation. Sulfate reduction was suppressed in the upper 5 cm, where oxygen, manganese, and iron reduction prevailed. Below this zone, sulfate reduction peaked but coexisted with microbial iron reduction. All Mn reduction was apparently coupled to iron and sulfide oxidation in the upper 6 cm. Below that level, a transient accumulation of iron monosulfide and pyrite implied that sulfate reduction increased during the 19th century because of anthropogenic atmospheric sulfur deposition. Sediment mixing through bioturbation was crucial for the cycling of Mn, Fe, and S, and estimates of biodiffusion coefficients were 0.02–0.3 cm^2 d^{-1}.

Through the mineralization of organic matter, aquatic sediments, whether lacustrine or marine, play a key role in liberating organic-bound nutrients to fuel primary production (e.g., Wollast 1991; Brooks and Edgington 1994). The oxidation of organic carbon (C_{org}) is coupled to the reduction of an array of electron acceptors, including oxygen, nitrate, manganese oxides, iron oxides, and sulfate or C_{org} may be mineralized to CO_2 and methane by methanogenesis. The processes are here listed in order of decreasing energy gain, corresponding approximately to their zonation with depth in a sediment (e.g., Froelich et al. 1979; Canfield et al. 1993*b*), although sometimes considerable overlap exists where two or more processes occur simultaneously. For example, methanogenesis and Fe reduction can both coexist with sulfate reduction (e.g., Kuivila et al. 1989; Canfield et al. 1993*b*). In addition to the direct significance for carbon oxidation and nutrient regeneration, the partitioning of carbon mineralization among the different pathways can have other effects on the ecosystem, including the emission of toxic hydrogen sulfide, methane ebullition, and the retention of phosphate in the sediment (Roden and Wetzel 1996; Roden and Edmonds 1997).

Previous work has suggested that, in lacustrine sediments, C_{org} oxidation is mostly coupled to oxygen respiration, sulfate reduction, and methanogenesis (Capone and Kiene 1988). Oxygen is used by bacteria in the oxidation of C_{org} and in the abiotic or bacterial oxidation of reduced inorganic species like Fe(II), Mn(II), and H_2S (Bak and Pfennig 1991; Urban et al. 1994). Oxygen is also used for respiration by

[1] Corresponding author (bot@biology.sdu.dk).

Acknowledgments

We thank captain Ron Smith and the crew of the R/V *Neeskay* for a nice cruise. Special thanks to Barbara J. MacGregor and Brett J. Baker for planning the cruise and skillful scientific and technical assistance during sampling and processing of the samples and to Erik R. Christensen, Universty of Milwaukee, for ^{210}Pb calculations. U.T. thanks David A. Stahl, Susan Fishbain, John Kelly, Bradley E. Jackson, Hidetoshi Urakawa, and others for an unforgettable stay at Northwestern University. Furthermore, we acknowledge the reviewers for their effort and constructive contribution to the manuscript.

This study was supported by NSF grant DEB-9615356 to D.A.S., the Danish National Research Foundation through the Danish Center for Earth System Science, and the Faculty of Science, University of Southern Denmark, Odense.

benthic fauna. In eutrophic lakes, O_2 respiration may be of limited importance, because an anoxic hypolimnion sometimes develops during the summertime, and, when O_2 is present, the penetration in to the sediment is restricted to a few millimeters (Holmer and Storkholm 2001). In oligotrophic Lake Michigan, by contrast, the hypolimnion is oxic yearround, and O_2 penetrates ~2 cm into the sediment at our study site, which suggests a significant role for organotrophic oxygen respiration (MacGregor et al. 2001).

Sulfate reduction in lake sediments is generally thought to be limited by low SO_4^{2-} concentrations (typically <0.5 mmol L^{-1}), compared with seawater (28 mmol L^{-1}). However, because of intensive sulfide reoxidation near the sediment surface, internal recycling is important, and SO_4^{2-} reduction rates are much higher than diffusional fluxes from the overlying water (Urban et al. 1994). Freshwater strains of sulfate-reducing bacteria exhibit a high affinity toward SO_4^{2-} (Ingvorsen and Jørgensen 1984), and several studies have shown that SO_4^{2-} reduction accounts for up to 10–35% of sediment C_{org} oxidation in lake sediments (Ingvorsen and Brock 1982; Kuivila et al. 1989; Urban et al. 1994). Overall, the significance of sulfate reduction should be regulated by a combination of factors, including the amount of reactive organic matter depositing through the zone of oxic respiration, the availability of sulfate, and the competition for organic matter by microbes that are using other electron acceptors, like Mn and Fe oxides (Sørensen 1982; Lovley and Phillips 1987, 1988). The availability of oxidized Fe and Mn is driven largely by bioturbation through its influence on the reoxidation of reduced Fe(II) and Mn(II) and the burial of oxidized Fe(III) and Mn(IV) (Canfield et al. 1993*b;* Kostka et al. 2002). Thus, the intensity of bioturbation might also be expected to exert an important control on relative magnitudes of the different anaerobic carbon mineralization pathways.

In many lake sediments, methanogenesis is the most important pathway, accounting for up to 90% of the total carbon mineralization (Oremland and Capone 1988). This process only dominates when electron acceptors for the more favorable processes are depleted, which allows the methanogens to compete for organic substrates or H_2 (e.g., Lovley and Klug 1986; Roden and Wetzel 1996).

Compared with a substantial number of studies that considered the significance of oxic respiration, sulfate reduction, and methanogenesis in lacustrine sediments, the significance of manganese and iron reduction have received scant attention. These processes (Fe reduction in particular) can be of major significance for carbon oxidation in marine and salt marsh sediments, as well as in freshwater wetlands (e.g., Canfield et al. 1993*a*; Roden and Wetzel 1996, 2002; Thamdrup 2000; Kostka et al. 2002). The potential importance of metal oxide reduction in lakes has been indicated by, for example, the mobilization of Mn^{2+} and the depth distributions of Fe(III) and Fe(II) (Aguilar and Nealson 1994; Kappler et al. 2004). The efficient recycling of reduced Mn and Fe is a prerequisite for the major contribution from Mn or Fe reduction to carbon oxidation, and important mechanisms that sustain such recycling include sediment bioturbation and oxygen injection through plant roots (e.g., Canfield et al. 1993*a*; Roden and Wetzel 1996, 2002; Thamdrup 2000; Kostka et al. 2002). In Lake Michigan, the amphipod *Diporeia* sp. dominates the benthic fauna and is found in densities up to 15,000 m^{-2}, with a lake mean of 5,240 m^{-2} (Nalepa et al. 2000). These detritivores ingest organic matter in subsurface sediment, thereby actively irrigating and reworking the upper sediment layers. Therefore, the prospect exists that metal oxide reduction could be a significant pathway of carbon mineralization in Lake Michigan sediments. The objective of the present study was to quantify rates and pathways of benthic carbon mineralization at a deep site in Lake Michigan. By doing so, we have come further in understanding how carbon mineralization is regulated in lacustrine settings. We focused on a site at 100 m depth that represents the average depth of Lake Michigan.

Materials and methods

Study site—Lake Michigan sediment was sampled in October 1999 at the Fox Point station (43°11′40″N, 87°40′11″W) 27 km northeast of Milwaukee, Wisconsin, which has previously been studied as representative of the open waters of the lake (e.g., Brooks and Edgington 1994). The water depth was 101 m, which is the average depth of the lake. The profundal zone extending from the 50-m isobath to the deepest part at 275 m depth covers 70% of the lake area. Temperature-driven mixing of the lake brings nutrients from the bottom to the euphotic zone during spring, where primary production is dominated by diatoms (Fahnenstiel and Scavia 1987). Overall, the lake is oligotrophic, with low rates of primary production (380 mg C m^{-2} d^{-1}; Eadie et al. 1984), but the southern and western parts are more productive than the northern and eastern parts because of nutrient supply from anthropogenically affected drainage areas and upwelling (e.g., Mackin et al. 1980; Nalepa et al. 2000). The bottom-water temperature varies seasonally from 1°C to 5°C and was 4.1°C at time of sampling. The bottom-water oxygen level is close to saturation, and penetration into the sediment is typically 2.1 ± 0.25 cm (±SD, $n = 11$) throughout the year (MacGregor et al. 2001). Bottom-water nitrate concentrations are 21–28 μmol L^{-1}, with nitrate penetrating slightly deeper than oxygen throughout the year, except when bottom- and pore-water concentrations briefly increase during spring (MacGregor et al. 2001). The sediment consisted of flocculent dark-brownish mud with black spots in layers below 10 cm. The porosity depth profile decreased from 0.95 to 0.90 in the upper 5 cm and decreased to 0.87 in the deepest layers. Sedimentation mass flux to the surface is 0.027 g cm^{-2} yr^{-1}, as calculated from unsupported excess ^{210}Pb depth distribution (Fitzgerald 1989; Hermanson and Christensen 1991), which, at the porosity at 17 cm depth ($\phi = 0.87$), corresponds to a sedimentation rate of 0.8 mm yr^{-1} (Hermanson and Christensen 1991). The upper ~5 cm is bioturbated by the burrowing activity of the amphipod *Diporeia* sp., which is the most abundant macrobenthos in the profundal lake. At the time of sampling, *Diporeia* was observed in densities of ~1,000 m^{-2}, compared with typical densities of 2,000–8,000 m^{-2} at 100 m depth (Nalepa et al. 2000).

Sediment was collected from the vessel R/V *Neeskay*

(University of Wisconsin) with a 900-cm^2 box corer and subsampled onboard in 6.79-cm (inner diameter) cores, which were immediately placed in an ice-water bath in the dark for transportation and stored at 4.5°C in a cooling room until further processing for sediment incubations the next day.

Sediment incubations—Total anaerobic mineralization rates and the relative contribution of oxic respiration, manganese reduction, iron reduction, sulfate reduction, and methanogenesis were determined by incubating 1-cm sediment intervals to 18 cm depth. Fourteen cores were sectioned in a N_2-filled glove bag, where sections from the same depth were pooled, mixed, and loaded into gas-tight plastic bags to a final volume of 300–400 ml (Hansen et al. 2000). The bags were incubated in larger N_2-filled storage bags (laminated ethyl-vinyl-alcohol; NEN/PE) to further ensure anoxia and were then subsampled on days 1, 2, 4, 8, and 18. All incubations were performed in the dark at close to the in situ temperature, 5.0°C. The sediment incubations were processed in an anoxic glove bag that rested on an ice-water bath, to minimize temperature artifacts. Sampling from each bag was initiated by subsampling 3 ml of sediment with a 3-ml cutoff syringe for the detection of CH_4 production. The sample was quickly transferred to a culture tube that was immediately stoppered with a butyl rubber septum and crimped. Activity was terminated by autoclaving for 20 min, and the tubes were stored at 5°C for later analysis. Two 15-ml centrifuge tubes per bag were filled completely with sediment—one was frozen at −20°C for later analysis of solid-phase Mn and Fe. Pore water was extruded from the other tube by centrifuging for 10 min at 2,000 *g*. The supernatant was filtered through 0.22-μm cellulose acetate filters (Lida Manufacturing) in a N_2-filled glove bag, and aliquots were distributed as follows: 1.8 ml in glass vials that were capped with Teflon-coated butyl rubber septa leaving no head space, stored at 5°C, analyzed for dissolved inorganic carbon (ΣCO_2) the next day, and subsequently stored frozen at −20°C for later analysis of NH_4^+; 1 ml in 1.5-ml eppendorf tubes that were immediately frozen at −20°C for later analysis of SO_4^{2-}; 2 ml in 2.2-ml cryovials, acidified with 6 mol L^{-1} HCl (1% vol), and stored for the later determination of dissolved Fe^{2+} and Mn^{2+}.

Sulfate reduction rates were determined at each sampling day by the ^{35}S-tracer technique (Jørgensen 1978); 5 μl (46 KBq) of carrier-free ^{35}S-SO_4^{2-} (ICN Pharmaceuticals) was injected into subsamples of sediment loaded in cutoff 5-ml plastic syringes that were subsequently plugged with butyl rubber stoppers. The syringes were incubated for 6–7 h in N_2-filled NEN/PE storage bags at 5.0°C, and the incubation was terminated by fixing sediment in 10 ml of 20% zinc acetate, and the mixture was frozen until analysis. Reduced ^{35}S was recovered by two-step distillation that divided reduced sulfide into acid-volatile sulfide (AVS; H_2S and FeS) by cold distillation in 6 mol L^{-1} HCl and then hot distillation in reduced chromium (CRS; S^0 and FeS_2; Fossing and Jørgensen 1989). Sulfate reduction rates were calculated according to the method of Jørgensen (1978) and background corrected by the subtraction of ^{35}S recovered from the distillation of sediment that had been fixed in zinc acetate immediately after the injection of the tracer. Rates are presented as the average of consecutive samplings.

The total sediment metabolism was determined from benthic exchange fluxes of four cores. Before the flux measurements, cores were preincubated close to in situ temperature at 4.5°C for 48 h while the overlying water was gently purged with air. After the removal of the air supply, samples of the overlying water were collected before capping with rubber stoppers and after incubation for 27 h (corresponding to a O_2 decrease to ~70% of saturation). The overlying water phase (~11 cm) was stirred with a rotating Teflon-coated stirring bar attached to the stopper and receiving momentum from an external rotating magnet at ~100 rpm. Samples for O_2 and ΣCO_2 were collected in 16-ml Hungate-type anaerobic culture tubes, leaving no head space. Oxygen samples were conserved by the addition of Winkler reagents and analyzed within 1 d, whereas ΣCO_2 samples were conserved by the addition of 0.2% saturated HgCl, and they were analyzed within 4 d. Samples for NO_3^-, NH_4^+, and SO_4^{2-}, were stored frozen in 20-ml vials.

Chemical analysis—Concentrations of NH_4^+, NO_3^-, ΣCO_2, and SO_4^{2-} in lake and pore water were analyzed as follows: NH_4^+, colorimetrically according to the salicylate method (SD, 0.24 μmol L^{-1}; Bower and Holm-Hansen 1980); NO_3^-, on a flow-injection analyzer according to the method of Grasshoff et al. (1983; Tecator; SD, 0.33 μmol L^{-1}); ΣCO_2, by flow injection/diffusion cell analysis with conductivity detection (SD, 24 μmol L^{-1}; Hall and Aller 1992); and SO_4^{2-}, by suppressed anion chromatography (Sykam; SD, 5.0 μmol L^{-1}). Oxygen was analyzed by the Winkler titration (SD, 2.2 μmol L^{-1}). Methane was measured with a gas chromatograph equipped with a flame ionization detector (Hewlett Packard 5890 series II; SD, 6.0 nmol cm^{-3}).

Solid-phase iron was extracted by anoxic acidic oxalate at pH 3 and by 0.5 mol L^{-1} HCl (Thamdrup et al. 1994). Soluble Fe^{2+} in pore water and extracts was determined with Ferrozine (Stookey 1970), whereas total Fe in extracts was determined after the reduction of Fe^{3+} with 1% (wt/wt) hydroxylamine hydrochloride. The concentration of solid-phase Fe(III) oxides was calculated as the difference between total Fe and Fe(II) in the oxalate extractions (Thamdrup et al. 1994). Particulate Mn was extracted with dithionite-citrate-acetic acid (DCA; pH 4.8; Lord 1980). Mn in extracts and soluble Mn^{2+} were determined by flame atomic absorption spectrometry (Perkin-Elmer 2380). All extractions were performed in 8 ml of extracting solution with 0.5 g thawed sediment, and extraction times were 1 h for HCl and DCA and overnight for oxalate (Thamdrup et al. 1994). Concentrations of sulfide in AVS and CRS extractions were determined by use of the methylene blue technique (Cline 1969). Adsorbed NH_4^+ was determined by the extraction of ~2.0 g wet sediment in 2 mol L^{-1} KCl at 5°C for 1 h and analyzed as described above. The dimensionless ammonium adsorption coefficient (*K*) was calculated according to the method of Mackin and Aller (1984):

$$K = \frac{(1 - \phi)}{\phi} \rho_s K^* \quad (1)$$

where ϕ is porosity, ρ_s is the dry density of the solid parti-

cles, and K^* is the amount of KCl extractable NH_4^+/pore-water NH_4^+ in ml g^{-1}. Total particulate nitrogen and carbon were determined from sediment dried at 105°C for 6 h and ground before analysis on a Carlo Erba 1100EA elemental analyzer (SD, 2%). Organic C and N in parallel samples were removed by combustion at 520°C for 6 h, and inorganic C and N were determined as above. Particulate organic C (POC) and N (PON) were calculated by difference of total and inorganic concentrations according to the method of Kristensen and Andersen (1987).

The sediment water content (β) in each layer was determined by oven drying to constant mass at 105°C; from this, porosity (ϕ) was calculated as $\beta/[(1 - \beta)/\rho_s + \beta]$, under the assumption of a bulk density of solids (ρ_s) of 2.45 g cm^{-3}.

Data analysis of process measurements—The rate of concentration change of dissolved pore-water constituents was calculated from the slope and the associated standard error of linear regression of successive time points. Only the first three to five and significantly linear ($p < 0.05$) time points were used. Sulfate reduction rates were calculated as means with standard error of the first four determinations in the time series.

Carbon oxidation rates for microbial processes using electron acceptors other than SO_4^{2-} were calculated as the difference between ΣCO_2 accumulation and ΣCO_2 production coupled to sulfate reduction rates. The latter was calculated under the assumption of a $\Sigma CO_2 : SO_4^{2-}$ stoichiometric ratio of 2 (Canfield et al. 1993*b;* Thamdrup and Canfield 1996).

Results

Carbon mineralization—As a result of organotrophic microbial activity, dissolved inorganic carbon and NH_4^+ accumulated during the bag incubations (Fig. 1A,B). Initial increases in dissolved inorganic carbon concentrations were approximately linear, but, after 8 d, the production tended to slow down in the surface layers (<3 cm), and in the deeper layers (>3 cm), ΣCO_2 concentration decreased slightly, which probably resulted from the precipitation of carbonates. Production rates of ΣCO_2 were calculated from the linear increases in concentrations, including three to five time points. The ΣCO_2 production rates decreased asymptotically with depth toward zero in the deepest layers (Fig. 2A). Ammonium was liberated at very low rates of <4.5 nmol cm^{-3} d^{-1} (Fig. 2B). The high ratio of ΣCO_2 to NH_4^+ accumulation rates was consistent with a high adsorption capacity of the sediment, as indicated by the adsorption coefficient of 18.3 ± 3.0 (±SE, $n = 18$). In general agreement with the depth distribution of mineralization rates, both POC and PON decreased with depth toward stable concentrations of recalcitrant organic matter that may be subject to permanent burial in the sediment (Figs. 2A, 3D). Inorganic carbon was practically constant with depth, with concentrations of 1.28–1.53 mmol g dw^{-1}.

The initial ΣCO_2 concentrations peaked at 1–3 cm depth and changed little below, whereas NH_4^+ concentrations peaked in the oxic zone and subsequently accumulated with depth in the anoxic sediment layers (Fig. 2A,B). However, these solute concentrations are affected by the irrigating activity of *Diporeia* sp.

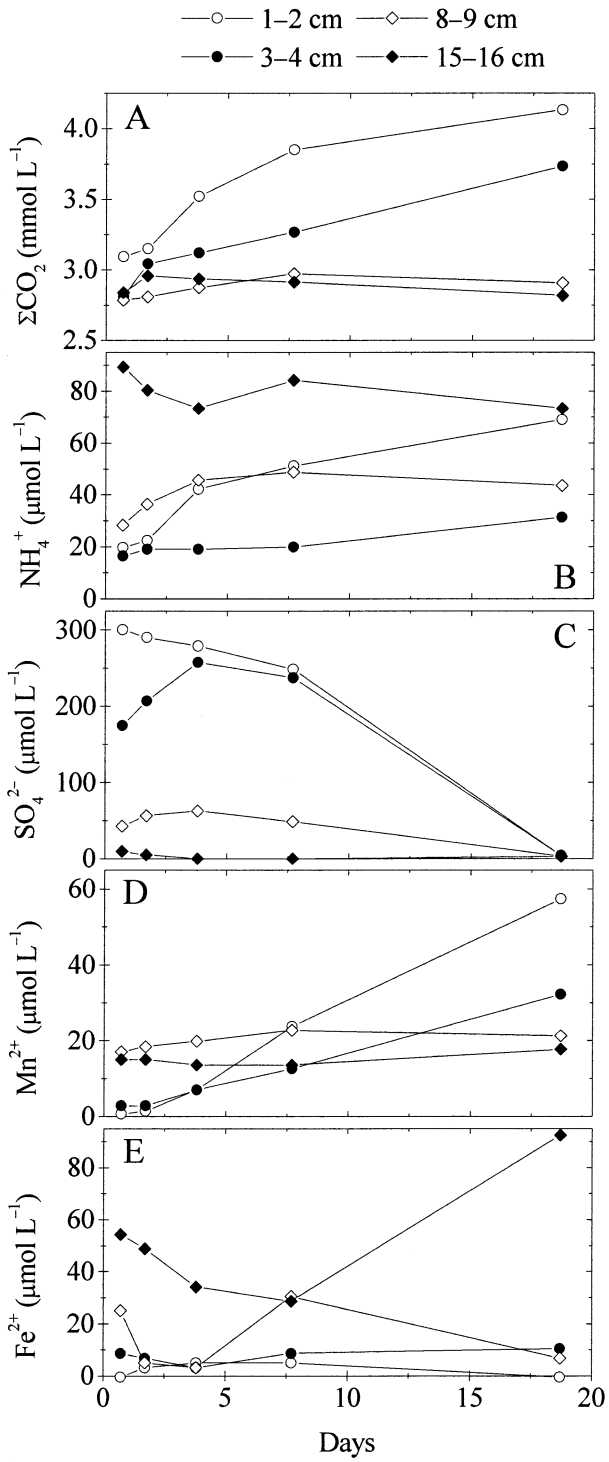

Fig. 1. Changes of pore-water constituents during anoxic incubations at four depths: (A) ΣCO_2, (B) NH_4^+, (C) SO_4^{2-}, (D) Mn^{2+}, and (E) Fe^{2+}.

Methanogenesis was insignificant with concentration changes of CH_4 of −1.1–0.63 nmol cm^{-3} d^{-1} in bag incubations (Fig. 2A), and concentrations were <85 nmol cm^{-3}

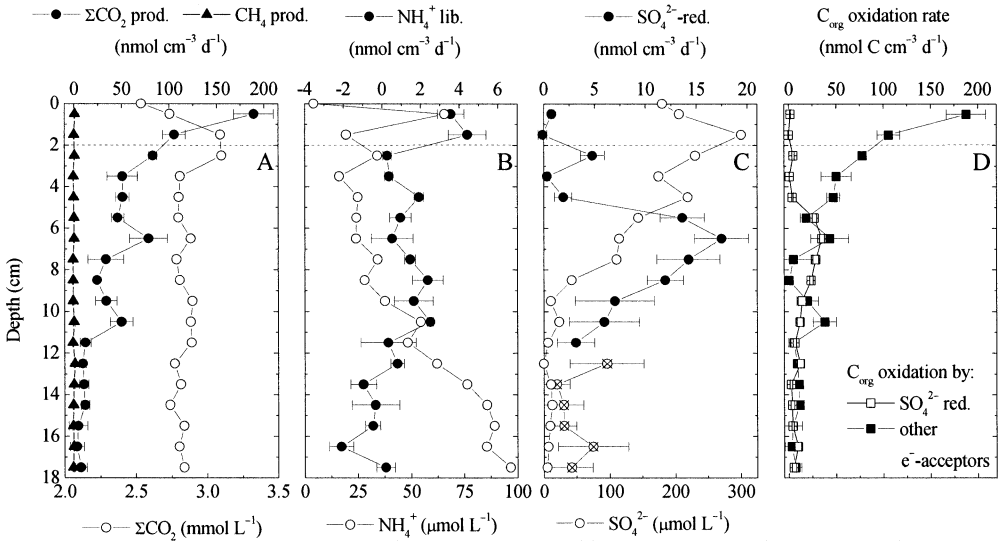

Fig. 2. Rates of anaerobic mineralization, methane production, and initial pore-water concentrations in bag incubations with discrete sediment horizons. (A) ΣCO_2 and (B) NH_4^+ accumulation rates were calculated from linear regressions with error bars indicating the SE, and (C) SO_4^{2-} reduction rates are means of four replicate measurements, with error bars indicating the SEM. SO_4^{2-} reduction below 13 cm depth (checked squares) are discounted because of the presence of residual unreactive pore-water SO_4^{2-} (*see text*). (D) C_{org} oxidation rates with electron acceptors other than SO_4^{2-} were determined as the difference between ΣCO_2 accumulation and SO_4^{2-} reduction rates converted to carbon units (*see text*). The dashed line represents the average O_2 penetration depth.

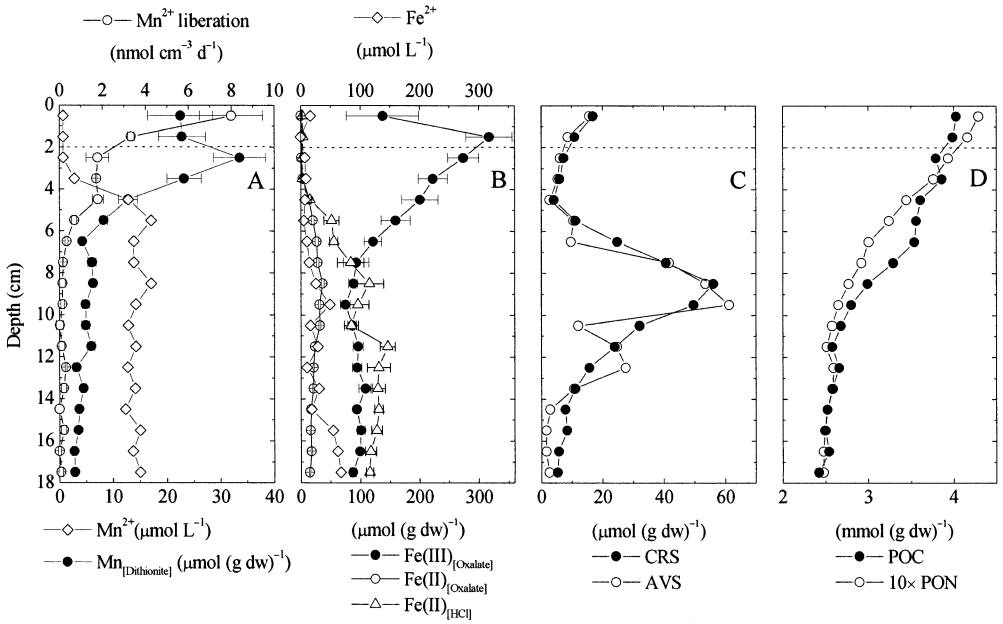

Fig. 3. Vertical depth distribution of (A) initial concentrations and liberation rates of dissolved Mn^{2+} and solid-phase Mn; (B) initial concentrations of dissolved Fe^{2+} and solid-phase Fe; (C) reduced solid-phase S; and (D) POC and PON. Liberation rates were calculated from linear regressions, with error bars indicating the SE. Solid-phase Mn and Fe are means of four replicate extractions in DCA, anoxic oxalate, and 0.5 mol L^{-1} HCl. The reduced sulfur pools, AVS and CRS, and POC and PON (multiplied by 15) are single determinations from initial sampling. The dashed line represents the average O_2 penetration.

(not shown). However, because of the possibility for degassing during the initial sediment handling, CH_4 concentrations may be underestimated.

Sulfate reduction—The SO_4^{2-} pore-water profile indicated net production in oxic sediment layers and depletion in deeper layers, to a residual concentration of <13 μmol L^{-1} below 13 cm depth (Fig. 2C). Sulfate reduction rates measured by the ^{35}S radiotracer technique in the anoxic bag incubations were in general accordance with the change in SO_4^{2-} concentrations during the first 8 d. Sulfate reduction was detectable in both oxic and anoxic layers, although rates in the oxic zone may be artifacts caused by the interruption of O_2 supply in the anoxic incubations (Fig. 2C). Sulfate reduction rates also agreed approximately with the depthwise depletion of pore-water SO_4^{2-}, and the rates paralleled the depth distributions of AVS and CRS (Fig. 3C). The rates peaked between 5 and 18 nmol cm^{-3} d^{-1} in a relatively broad zone extending from 5 to 13 cm depth (Fig. 2C). Turnover of the $^{35}SO_4^{2-}$ tracer also occurred below 13 cm, although SO_4^{2-} here was depleted to a residual concentration that continued to be present during the incubations. Hence, this SO_4^{2-} pool was most likely not reactive, and these rates are not considered to be realistic and were therefore discounted. Similar unreactive residual SO_4^{2-} pools have been found in other oligohaline sediments (Bak and Pfennig 1991; Roden and Tuttle 1993; Roden and Wetzel 1996).

Under the assumption of an overall stoichiometry of 2 mol CO_2 to 1 mol SO_4^{2-} for C_{org} oxidization by sulfate reduction (Westrich and Berner 1984; Thamdrup and Canfield 1996), SO_4^{2-} reduction accounted for $<7\%$ of ΣCO_2 production in the upper 5 cm and below 13 cm, whereas, in the midzone at 5–13 cm, sulfate reduction constituted 25–100% of carbon oxidation (Fig. 2D).

Mn and Fe reduction—Concentrations of extractable Mn were highest at 0–4 cm depth, with a peak just below the depth of O_2 and NO_3^- penetration, and concentrations decreased to a background level at 7 cm depth (Fig. 3A). This distribution, in concert with a distribution of dissolved Mn^{2+} increasing from <1 μmol L^{-1} to 17 μmol L^{-1} in the lower part of the Mn-enriched zone (Fig. 3A), suggests the intensive recycling of Mn oxides. Manganese remaining below this zone likely represents nonreactive Mn and possibly authigenic Mn(II). Accordingly, dissolved Mn^{2+} concentrations increased linearly during bag incubations, indicating the reduction of Mn oxides. Liberation rates were highest in the top sediment layer and decreased asymptotically, reaching zero at the same depth of $\sim$6 cm, where background levels of extractable Mn were reached (Figs. 1D, 3A).

Poorly crystalline Fe(III) oxides were $\sim$10 times more abundant than extractable Mn, with a peak of 320 μmol (g dw)$^{-1}$ in the lower oxic zone and with concentrations decreasing steeply to a background level of $\sim$90 μmol (g dw)$^{-1}$ below 8 cm depth (Fig. 3B). Below 4 cm depth, reduced Fe(II) accumulated in both oxalate and HCl extractable fractions to 37 and 131 μmol (g dw) $^{-1}$, respectively. The results are mean values of four replicate extractions from each depth interval. The variability of the Fe analyses was too large to permit a direct determination of Fe reduction rates from changes in the Fe(II) and Fe(III) pools, as has been done with more active freshwater sediment (Roden and Wetzel 1996). Dissolved Fe^{2+} increased from $\sim$7 μmol L^{-1} in the upper 6 cm to 67 μmol L^{-1} in the deepest layer (Fig. 3B), but concentrations did not change uniformly during the incubations, probably because of both adsorption and precipitation during Fe^{2+} liberation (Fig. 1E).

Table 1. Directly measured sediment fluxes and depth-integrated rates from the bag incubations.

	Measured fluxes, rate$\pm$SE (n) (mmol $m^{-2}d^{-1}$)	Depth-integrated rates, rate$\pm$SE* (mmol $m^{-2}d^{-1}$)
O_2	-5.7 ± 1.7 (4)	—
ΣCO_2	6.8 ± 1.8 (3)	8.0 ± 0.5
NO_3^-	0.54 ± 0.02 (4)	—
NH_4^+	0.10 ± 0.02 (4)	0.18 ± 0.03
SO_4^{-2}	0.69 ± 0.19 (4)	-0.78 ± 0.04

* The error term is the depth-weighted square root of the sum of squares of SEs for each of the 18 bag incubations.

Sediment-water exchange—Measured fluxes of ΣCO_2 and O_2 were of equal magnitude (Table 1). The directly measured flux of ΣCO_2 was not significantly different ($p > 0.05$; Student's t-test) from the depth-integrated rates compiled from the bag incubations, which implies that, overall, microbial activity was neither hampered nor stimulated by the sediment handling. Nitrogen was recycled from the sediment back to the water column mainly as NO_3^-, with an efflux that was four times higher than the efflux of NH_4^+. The concentrations of NO_3^- and NH_4^+ in the overlying water were 28 and 4 μmol L^{-1}, respectively. Also, sulfur was exported from the sediment as SO_4^{2-} concurrently with the consumption of SO_4^{2-} by sulfate reduction within the sediment, which implies that, at the time of sampling, sulfate production in the sediment exceeded sulfate reduction, as was also indicated by the sulfate distribution (Fig. 2C; *see also "Discussion"*). The concentration of SO_4^{2-} in the overlying water was 180 μmol L^{-1}. The flux of CH_4 was insignificant as it was not detectable within the applied sampling with a detection limit of 0.02 mmol m^{-2} d^{-1}.

Discussion

Carbon mineralization—The rate of total sediment metabolism determined directly from flux measurements of O_2 and ΣCO_2 are, to our knowledge, the first reported for profundal Great Lake sediments (Table 1). These are about half of rates measured in an 86-m-deep eutrophic lake (Urban et al. 1997) and are comparable to marine sites of $\sim$100-m water depth (Grant et al. 1991; Devol and Christensen 1993). From the sediment accumulation rate calculated from excess ^{210}Pb profiles, and assuming that carbon mineralization is complete at 18 cm depth, C_{org} burial was 1.8 mmol C m^{-2} d^{-1}. The flux of C_{org} to the lake floor can be estimated as burial plus ΣCO_2 efflux (Canfield 1994) and equaled 8.6 mmol C m^{-2} d^{-1} (Table 1). Thus, 21% of this flux was permanently buried in the sediment, which compares to marine

Table 2. Decay of organic matter (G') in the upper bioturbated (b) and the underlying (u) zone. Details of the calculations are given in the text. Note that rates and concentrations are relative to solid sediment volumes.

Depth interval (cm)	G' (μmol cm_s^{-3})	R (ΣCO_2) (μmol cm_s^{-3} yr^{-1})	k' (yr^{-1})	$\tau_{1/2}$ (yr)
0–2 (b)	95	1,035	11	0.06
2–6 (b)	710	249	0.4	2.0
6–18 (u)	3,150	74	0.02	30

sediments of similar sedimentation rates (Canfield 1994). The primary production in Lake Michigan has been estimated to be 32 mol C m^{-2} d^{-1} (Eadie et al. 1984), and the benthic C_{org} flux corresponded to 27% of this phytoplankton biomass production, which indicates that the sediment accounts for a significant part of the energy flow in the lake. Both seasonal and regional variations in benthic respiration are expected, and down-slope transport of both aquatic- and land-derived organic matter from shallow areas is also a source of carbon to deep Lake Michigan sediment (Meyers et al. 1980; Meyers and Eadie 1993). Thus, a wider survey is needed for an accurate determination of the role sediments in the lacustrine carbon cycle.

The close similarity of the measured efflux of ΣCO_2 and the integrated rate of carbon mineralization obtained from the bag incubations (Table 1) suggests that the anoxic bag incubation technique provided an accurate determination of mineralization rates across oxic and anoxic sediment layers, with no indication of the stimulation of microbial activity that is sometimes observed with bag incubations (Hansen et al. 2000). The carbon oxidation rates decreased exponentially with depth, which indicates that the rates, like in marine sediments, are determined by the concentration and reactivity of the organic carbon (Berner 1980*a*; Westrich and Berner 1984).

In the mixed sediment, fresh and older debris are mixed by bioturbation, which, as is discussed below, affects the sediment to ~6 cm depth. However, first-order rate constants of C_{org} oxidation can be approximated by assuming that distinct pools of organic matter, G_i', are oxidized successively in discrete zones by first-order kinetics—that is, G_1' with the apparent rate constant k_1' is oxidized in the oxic zone at 0–2 cm, G_2' with k_2' in the anoxic zone at 2–6 cm, and G_3' with k_3' in the deeper layers. The concentration of C_{org} oxidized in each zone, G', is determined as the difference between the POC concentration in the top and that in the bottom of each zone. Apparent first-order constants can then be calculated according to $R_i(\Sigma CO_2) = k_i' \times G_i'$, where $R_i(\Sigma CO_2)$ is the ΣCO_2 production and G_i' is the fraction of C_{org} oxidized. The results are given in Table 2 and illustrate that carbon reactivity decreased dramatically with depth by more than two orders of magnitude, as has been seen in marine sediments (Berner 1980*b;* Westrich and Berner 1984). The half-life ($\tau_{1/2}$) of G_1' in the oxic zone was comparable to that of C_{org} determined from offshore sediment traps in the hypolimnion of Lake Michigan (Meyers and Eadie 1993), and it approached that of the decomposition of fresh plankton (Westrich and Berner 1984). In our setup, entombed infauna potentially contributed to G_1', although the similarity of rates from whole cores and bag incubations suggested that this was not an important factor. The computation of k_1' ignores contributions of G_2' and G_3' to ΣCO_2 production in the k_1' horizon, but if we assume the same oxidation rates of k_2' and k_3' as in the deeper horizon, these together accounted for only ~3% of the activity at 0–2 cm.

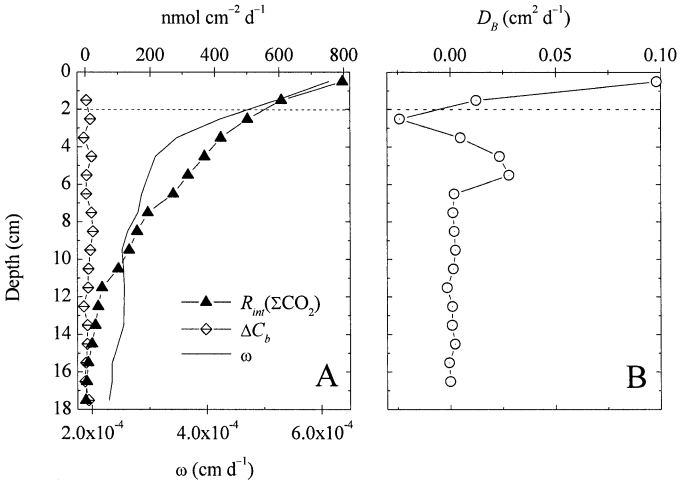

Fig. 4. (A) Depth dependence of $R_{int}(\Sigma CO_2)$ (integrated ΣCO_2 production rate from depth x to 18 cm), ΔC_b (change in burial flux of C_{org}), and ω (sediment burial rate). (B) Depth dependence of calculated biodiffusion coefficient, D_B. The dashed line represents the average O_2 penetration. See text for details.

According to the sediment accumulation rates (Fig. 4), the age of the sediment in the mixed zone is up to 50 yr. Comparison of this to a $\tau_{1/2}$ of 2 yr for k_2' C_{org}, emphasizes how the transport of relatively fresh organic debris from the surface to 6 cm depth by bioturbation is necessary for sustaining the measured activity to this depth. Below the mixed zone, the k_3' was comparable to values obtained for organic matter at similar depths in marine sediments (Berner 1980*b;* Westrich and Berner 1984).

Pathways of carbon oxidation—Rates of carbon oxidation coupled to the different electron acceptors can be quantified by considering the vertical distribution of O_2, NO_3^-, and Mn and Fe oxides (Fig. 3) and comparing these to the excess ΣCO_2 production not accounted for by SO_4^{2-} reduction (Canfield et al. 1993*b*; Thamdrup and Canfield 1996). Total rates of carbon oxidation can also be estimated from NH_4^+ accumulation rates, overcoming a possible underestimation of ΣCO_2 production due to the precipitation of carbonates (Canfield et al. 1993*b*). However, because of a very high ammonium adsorption coefficient compared with marine sediments (Mackin and Aller 1984), liberation rates of NH_4^+ were small, making this approach inaccurate.

The analysis revealed that >60% of the total carbon oxidation was channeled through anoxic pathways (Table 3). Within the oxic zone, O_2 is used for respiration by bacteria and eukaryotes, including meiofauna and *Diporeia* sp., and, as discussed below, a significant part is consumed by the reoxidation of reduced chemical species. As was estimated

Table 3. Depth-integrated rates of carbon oxidation coupled to the reduction of different electron acceptors. Oxidation rates with O_2 and Fe(III) are determined from the difference of SO_4^{2-} reduction and total carbon oxidation rates in the oxic and anoxic zones, respectively. See text for details.

Microbial process	Interval (cm)	Rate* (mmol C $m^{-2}d^{-1}$)	%†
Oxic respiration	0–2	2.95±0.24	37
Fe reduction	2–18	3.52±0.38	44
Sulfate reduction	2–13	1.56±0.08	19
Methane net rate	2–18	−0.1±0.02	0.9

* The error term is the depth-weighted square root of the sum of squares of SE.

† Percentage of total carbon oxidation.

from NO_3^- gradients (data not shown), the contribution of denitrification was <3% of the ΣCO_2 production, which resembles contributions determined from continental marine sediments (Thamdrup 2000).

The distributions of particulate and soluble Mn and the liberation of Mn^{2+} to 6 cm depth during incubations (Fig. 3A) indicated that Mn-reducing bacteria could contribute to carbon oxidation. However, as is discussed in more detail below, further analysis indicated that Mn oxide reduction was predominantly coupled to the reoxidation of reduced iron and sulfur. Any direct contribution of Mn reduction to carbon oxidation is therefore contained in our estimate of Fe reduction.

Microbial iron reduction was the dominant carbon oxidation pathway within the anoxic sediment zone, contributing as much to total C_{org} oxidation, 44%, as processes within the oxic zone (Table 3). There was a good agreement between the distributions oxalate-extractable Fe(III) and the rates of carbon oxidation that were not coupled to sulfate reduction (Figs. 1D, 2B). Sulfate reduction was strongly suppressed to 5 cm depth, where oxalate-extractable Fe(III) was ≥200 μmol (g dw) $^{-1}$, whereas sulfate reduction rates increased as Fe(III) was depleted below this concentration. This apparently limiting Fe(III) concentration corresponded to 49 μmol Fe(III) cm^{-3} at the porosity of 0.9 found at 5 cm depth. If the ~90 mol (g dw)$^{-1}$ Fe(III) found throughout the deeper layers (Fig. 2B) represents an unreactive background that is present at all depths, the limiting concentration is reduced, by subtraction of this background, to 27 μmol reactive Fe(III) cm^{-3}. The observed dependence of Fe reduction on Fe(III) concentrations is in good agreement with previous studies with both freshwater and marine sediments that have shown that this pathway requires 30–50 μmol poorly crystalline Fe(III) cm^{-3} to efficiently out-compete sulfate reduction or methanogenesis (Thamdrup 2000; Roden and Wetzel 2002; Jensen et al. 2003).

In profundal sediments of Lake Constance, Germany, Kappler et al. (2004) identified a zone of microbial iron reduction at ~1–4 cm depth, based on the distribution of O_2, Fe(III), and Fe(II). No process rates were measured at this site, but a general similarity of the redox zonation to that found in the present study suggests that microbial Fe reduction may also be an important contributor to carbon oxidation in Lake Constance. Higher most-probable-number counts of humic-reducing bacteria than of Fe-reducers in the sediment led to the suggestion that much Fe was reduced by humics serving as electron shuttles between bacteria and iron oxides (Kappler et al. 2004). This mechanism could also contribute to Fe reduction in Lake Michigan.

The inventory of reactive Fe(III), determined by subtracting the background concentrations of Fe(III) in oxalate extractions, was 770 mmol m^{-2}. At an integrated rate of microbial Fe reduction of 14.1 mmol Fe m^{-2} d^{-1}, derived from the rate in C_{org} equivalents (Table 3) under the assumption of a 4:1 Fe(III):C_{org} reaction ratio for the process (Roden and Wetzel 1996), we obtained a turnover time for Fe(III) by microbial iron reduction of 55 d. This value is similar to those estimated from coastal and continental slope marine sediments (Canfield et al. 1993*b*; Thamdrup and Canfield 1996). From the sediment accumulation rate and the Fe concentration at the surface, a delivery flux of 0.1 mmol Fe m^{-2} d^{-1} was estimated. Relating this to the iron reduction rate, we estimate that each Fe-atom is recycled, on average (14.1/0.1), 141 times before final burial in the sediment. Mechanisms of recycling necessary for sustaining the high Fe oxide concentrations required by Fe-reducing bacteria, through broad horizons of anoxic sediment, include intensive reoxidation driven by bioturbation, O_2 leaching from macrophyte roots, or both (Canfield et al. 1993*b*; Roden and Wetzel 1996; Kostka et al. 2002), as well as by the physical reworking of sediments by waves and currents (e.g., Aller et al. 1991). Estimates of bioturbation intensity in the lake sediment are provided below.

Sulfate reduction was a significant carbon oxidation pathway, despite low SO_4^{2-} concentrations, and contributed 19% of total sediment metabolism (Table 3), which is comparable to other hypolimnetic sediments (Ingvorsen and Brock 1982; Kelly and Rudd 1984; Kuivila et al. 1989). The activity of sulfate-reducing bacteria peaked at 5–13 cm depth and there equaled the contribution from microbial iron reduction, which implies that iron- and sulfate-reducing bacteria coexisted.

The kinetics of microbial SO_4^{2-} reduction can be approximated by Michaelis-Menten kinetics:

$$v = \frac{V'a}{K'_m + a} \tag{2}$$

where v is the SO_4^{2-} reduction rate, V' is the apparent maximum reduction rate, a is the concentration of SO_4^{2-}, and K'_m is the apparent half-saturation constant. Nonlinear regression of SO_4^{2-} reduction rates against SO_4^{2-} concentrations yielded a K'_m of 30 ± 13 μmol L^{-1} (±SE). However, this must be regarded as an upper estimate because of a potential influence of decreasing C_{org} availability with depth on sulfate reduction rates. Our K'_m is, however, similar to values from other freshwater sediments (Roden and Tuttle 1993; Urban et al. 1994), although it is higher than the K_m of 5 μmol L^{-1} determined for pure cultures of the freshwater sulfate reducer *Desulfovibrio vulgaris* (Ingvorsen and Jørgensen 1984). This general difference may be explained by a range of SO_4^{2-} affinities in the natural population of sulfate reducers.

The electron acceptor responsible for the low rates of ΣCO_2 production below 13 cm could not be determined with

certainty. The absence of methanogenesis in the deeper part of the investigated sediment layers suggested that iron- or sulfate-reducing bacteria were still active and efficiently outcompeted methanogenic bacteria (Ingvorsen and Jørgensen 1984; Lovley and Phillips 1987; Chidthaisong and Conrad 2000). Sulfate reduction was not a likely candidate, because, at these depths, sulfate was depleted to a stable background level, and, during the incubations, ΣCO_2 production was not balanced by sulfate consumption (Fig. 2C; *see also "Results"*). Although no gradient in extractable Fe(III) was observed, the liberation of Fe^{2+} to the pore water (Fig. 1E) indicated a possible involvement of Fe reduction. In addition to the extracted Fe(III), Fe(III) in crystalline oxides or clays may also support Fe reduction (Kostka and Luther 1994; Kostka et al. 1999).

Bioturbation and Fe cycling—On reduction in anoxic sediment layers, dissolved Fe^{2+} and Mn^{2+} are liberated and transported toward the oxic zone by diffusion or irrigation and here reoxidized, forming solid metal oxides (Fig. 3A,B). Furthermore, a large fraction of Fe(II) and Mn(II) is adsorbed to particles or bound in solid phases in, for example, carbonates or sulfides, which are transported to the oxic zone by the reworking activity of infauna. Besides bioturbation, some particle reworking may also occur by resuspension events during thermal mixing of the lake (Eadie et al. 1984).

The transport of Mn, Fe, and S within the sediment can be quantified under the assumption of a diffusional movement of sediment particles described by a biodiffusion coefficient (D_B), which can be estimated from mass-balance calculations based on depth distributions and reaction rates of solid components. Thus, at steady state, the vertical flux of C_{org} at a given depth within the sediment equals the sum of underlying C_{org} oxidation and permanent burial of C_{org}. The consumption of C_{org} supported by the burial flux of C_{org} in a given depth interval is equal to the difference in burial flux (ΔC_b) at the top and bottom of this interval (e.g., Boudreau 1997):

$$\Delta C_b(x1, x2) = B_{x1}(1 - \phi_{x1})\omega_{x1} - B_{x2}(1 - \phi_{x2})\omega_{x2} \quad (3)$$

where ϕ is porosity, B is the concentration of C_{org} in solids, and ω the sediment accumulation rate in cm yr^{-1} (Berner 1980*b*):

$$\omega = \frac{\Re}{\rho_s(1 - \phi)} \quad (4)$$

where $\Re$ is the rate of sediment flux to the surface, here 0.027 g cm^{-2} yr^{-1}, and ρ_s is the bulk density of 2.45 g cm^{-3}. In the upper sediment layers, the contribution of ΔC_b to the depth-integrated ΣCO_2 production rate, $R_{int}(\Sigma CO_2)$, was negligible, whereas burial could support the low carbon mineralization rates measured in the deepest layers ($\Delta C_b < 25$ nmol cm^{-2} d^{-1}; Fig. 4A). Thus, bioturbation strongly dominated the POC flux near the sediment surface, whereas it was of little importance deeper in the sediment. Using an approach similar to that of Berner and Westrich (1985) and Thamdrup et al. (1994), a biodiffusion coefficient (D_B) can be estimated from the difference between ΔC_b and $R_{int}(\Sigma CO_2)$. At steady state, the C_{org} oxidation rate supported by the diffusive flux of C_{org} in a given depth interval is the difference between the flux in at the top and the flux out at the bottom (e.g., Boudreau 1997):

$$R_{bio}(\Sigma CO_2)(x1, x2) = (1 - \phi_{x2})D_{B,x2}\left(\frac{dB}{dx}\right)_{x2} - (1 - \phi_{x1})D_{B,x1}\left(\frac{dB}{dx}\right)_{x1} \quad (5)$$

and, thus,

$$R_{int}(\Sigma CO_2) = \Delta C_b + R_{bio}(\Sigma CO_2) \quad (6)$$

Consistent with the good agreement between the measured C_{org} oxidation rate and the supported burial in the deepest sediment layers (Fig. 4A), we assume that $D_B(L) = 0$, where $L = 17$ cm—that is, the bottom of the deepest section analyzed. Thus,

$$R_{bio}(\Sigma CO_2)(x, L) = -(1 - \phi_x)D_{B,x}\left(\frac{dB}{dx}\right)_x \quad (7)$$

and inserting into Eq. 6 and rearranging:

$$D_B(x) = \Delta C_b(x, L) - \frac{R_{int}(\Sigma CO_2)}{(1 - \phi)\left(\frac{dB}{dx}\right)_x} \quad (8)$$

Values of D_B calculated this way are shown in Fig. 4B and indicate decreasing mixing with depth to 6 cm, where D_B was <0.002 cm^2 d^{-1}. A single negative D_B in the mixed layer was caused by a slight wobble in the profile of C_{org} (*see Fig. 3D*) and emphasizes the sensitivity of the approach to small inaccuracies in C_{org} determination. The sediment mixing coefficients are in accordance with previous determinations from depth distributions of ^{210}Pb and ^{137}Cs activity in the upper 2 cm of a comparable sediment in Lake Huron (Christensen and Bhunia 1986) and are also in accordance with the general relationship between D_B and burial velocity (ω) from aquatic environments (Boudreau 1994). Furthermore, the mixing depth approximates the average mixing depth in Lake Michigan of ~4 cm (Robbins and Edgington 1975) and corresponds to the depth where AVS and CRS started to accumulate and Mn^{2+} liberation ceased, which implies that Mn oxides have been depleted (Fig. 3A,C).

Analysis of the ^{210}Pb distribution at the Fox Point site was performed by Fitzgerald (1989), and on the basis of these data, D_B can be estimated by using a steady-state constant porosity model (Eq. 9), as described by Mulsow et al. (1998). Linear regression after log transformation of the excess ^{210}Pb distribution yielded a minimum D_B of 0.07 cm^2 d^{-1} in the upper 3 cm (slope − 1 SD), and $D_B < 0.001$ cm^2 d^{-1} in the deeper zone to 8 cm. Hence, a nearly similar trend and similar magnitudes of mixing coefficients were obtained, compared with the D_B estimates based on C_{org} flux and oxidation rate.

In the mixed zone from 1 to 6 cm depth, steep gradients of Mn and Fe(III) indicated considerable reduction rates, and, using a mean of the positive D_B values (Fig. 4) while assuming that mixing coefficients of POC and metal oxide–containing minerals are the same, fluxes can be calculated from the concentration gradients (Boudreau 1997):

Table 4. Calculated average biodiffusion coefficient (D_B; Eq. 8, $n=4$) in the mixed layer, based on ΣCO_2 production and C_{org} distribution. Fluxes (J_B) of C_{org} and solid-phase Mn, Fe, and S are calculated from linear regression of the maximum gradients in the mixed zone at 1–6-cm depth and were compiled according to Eq. 9.

Depth interval (cm)	D_B ($cm^2 d^{-1}$)	$Fe(II)_{HCl}$+CRS		$Fe(III)_{oxalate}$	
		Mn_{DCA}	(mmol $m^{-2} d^{-1}$)		C_{org}
1–6	0.017	−0.361	0.881	−1.348	−3.367

$$J_B = -(1 - \phi)D_B\left(\frac{dB}{dx}\right) \quad (9)$$

The resulting fluxes of solid phase Mn, Fe(III), Fe(II), reduced sulfur compounds, and POC are given in Table 4. Concentrations of Fe(II) were calculated as $Fe(II)_{HCl}$ + 0.5 × CRS, which assumes that all CRS represented pyrite, FeS_2. Pyrite is not extracted by the HCl extraction.

The reduction of Fe(III) estimated from the gradient approximately balanced the Fe(II) production (Fig. 3B, Table 4). These Fe fluxes were three to four times lower than both the calculated C_{org} flux and the integrated carbon oxidation rate coupled to iron reduction (Table 3). This ratio is not in agreement with the 4 : 1 ratio of $Fe(III) : CO_2$ expected for organotrophic iron reduction (Roden and Wetzel 1996).

This discrepancy could also be illustrated through calculations of biodiffusion coefficients based on the Fe(III) distributions and microbial iron reduction rates similarly to those described for C_{org} distributions and C_{org} oxidation rates (Eqs. 3–8). The depth distribution of iron reduction rates was derived from the rates of carbon oxidation not coupled to sulfate reduction in the 2–10 cm depth interval (Fig. 2D) under the assumption of a $4 : 1$ $Fe(III) : CO_2$ ratio for this type of respiration (Roden and Wetzel 1996). The calculations yielded values of D_B of 0.11–0.31 $cm^2\ d^{-1}$ to 9 cm depth. Several factors may contribute to the discrepancy between C_{org}- and Fe(III)-based D_B values: iron gradients may be influenced by reoxidation below the stable oxic/anoxic interface, iron may be transported by other mechanisms than C_{org}, or our steady-state assumptions may not be valid for the depth distribution of the solid species. A non-steady-state is indicated for sulfur diagenesis (see below), and this factor is likely to explain much of the discrepancy.

Cycling of Mn and S—Below the oxic zone, Mn oxides are suitable electron acceptors for both microbial carbon oxidation (Thamdrup 2000) and the abiotic oxidation of reduced iron and iron sulfides, FeS and FeS_2 (Postma and Appelo 2000; Schippers and Jørgensen 2001). The lack of accumulation of Fe(II), AVS, and CRS in the anoxic, Mn-enriched zone from ~2 to 4 cm suggested that the oxidation of Fe(II) and sulfides could be coupled to Mn oxide reduction (Fig. 3A,C). Comparison of the calculated fluxes of Mn, and $Fe(II)_{HCl}$ + CRS (Table 4) shows that Mn oxides in the mixed zone could be used exclusively for abiotic reoxidation of Fe(II) and iron sulfides. Such a conclusion has also been reached for several marine sediments (Canfield et al. 1993*b*; Aller 1994). The residence time of SO_4^{2-} in the sediment with respect to reduction was only 21 d (SO_4^{2-} inventory/SO_4^{2-} reduction rate), but the net efflux equaled the SO_4^{2-} reduction rate (Tables 1, 3), which implies that reoxidation was extremely efficient and was twice as fast as consumption. The observed SO_4^{2-} efflux cannot be a persistent phenomenon but suggests that AVS and CRS pools may have accumulated during spring and summer and are reoxidized and recycled back to the water column during fall. This emphasizes that bioturbation is also important for sulfur diagenesis and supports SO_4^{2-} reduction as a significant carbon oxidation pathway in deeper sediment layers. McKee et al. (1989) observed similar non–steady-state Mn^{2+} pore water distributions in Lake Superior during the same period. However, seasonal studies in Lake Michigan are needed to further elucidate the diagenesis and burial of Mn, Fe, and S and possible fluctuations in their relative role as electron acceptors for the microbial decomposition of organic matter.

Below the sediment mixing depth, both AVS and CRS accumulated where SO_4^{2-} reduction was active (Figs. 2C, 3C). The decrease in AVS and CRS toward greater depths cannot be explained by reoxidation. Instead, the full depth distribution can be interpreted as evidence of stimulated SO_4^{2-} reduction during the past ~200 yr, which implies that SO_4^{2-} reduction rates were low and approximately balanced with reoxidation rates at the beginning of the industrial revolution, in the 18th century (Mitchell et al. 1988). At this time, the open-water SO_4^{2-} concentrations were ~60 μmol L^{-1}, but they increased during the 19th century, to modern concentrations of 180–250 μmol L^{-1} (data extracted from STORET, Environmental Protection Agency, USA; http://www.epa.gov/storet/ and Beeton 1969), which may have stimulated SO_4^{2-} reduction, leading to higher accumulation rates of FeS and FeS_2. Allochthonous SO_4^{2-} may derive from anthropogenic atmospheric S deposition (e.g., Mitchell et al. 1988). Increasing SO_4^{2-} reduction rates are known to enhance the release of PO_4^{3-} in lake sediments, which may further contribute to eutrophication of the lake (Roden and Edmonds 1997).

In conclusion, our study shows that microbial Fe reduction can be a major respiratory process in profundal lake sediments, contributing 44% of the carbon oxidation in the present case. The important prerequisites for this contribution are (1) a high content of iron involved in redox cycling; (2) a moderate flux of organic matter, with little more than an unreactive residue remaining at the bottom of the Fe reduction zone; and (3) intense bioturbation of the sediment to ~6 cm depth, which recycles Fe(II) to oxidation and buries reactive organic matter and Fe(III) in the anoxic sediment. Bioturbation was also important for the cycling of Mn and S. The role of the manganese cycle appeared mainly to be a shuttling of electron equivalents from Fe(II) and reduced S to oxygen, whereas sulfate reduction, although suppressed

above 5 cm depth, accounted for 19% of the carbon oxidation. As a result of the efficient coupling of carbon oxidation to Fe and sulfate reduction, methanogenesis was insignificant, and the partitioning of carbon oxidation among terminal electron acceptors resembled marine continental shelf sediments and contrasted with many freshwater sediments, where methanogenesis is an important pathway (Oremland and Capone 1988; Thamdrup 2000).

The profundal sediment is an important compartment in the carbon cycle of the lake. Thus, the input of C_{org} to the sediment corresponded to 27% of the primary production, and the half-life of organic matter mineralized in the oxic zone was 0.06 yr, which was similar to mineralization during sinking through the water column. Below the bioturbated zone, carbon oxidation kinetics were more than two orders of magnitude slower, and 21% of the organic matter that reached the lake floor was permanently buried.

The amphipod *Diporeia* sp. appears to be an important agent for the bioturbation and to profoundly influence the biogeochemistry of carbon, manganese, iron, and sulfur. Densities of *Diporeia* in Lake Michigan have decreased during recent decades, presumably owing to competition for food sources from the invading filter-feeding mussel *Dreissena polymorpha*, which inhabits nearshore sediments (Nalepa et al. 1998; Madenjian et al. 2002). A decrease in bioturbation intensity brought by from decreasing numbers of *Diporeia* might substantially alter the partitioning of carbon oxidation pathways in the sediment, in particular diminishing the role of iron reduction and possibly favoring methanogenesis. We cannot presently predict such changes with any accuracy, but this perspective emphasizes the variety of the information needed to understand the regulation of carbon oxidation pathways in any given sediment.

References

AGUILAR, C., AND K. H. NEALSON. 1994. Manganese reduction in Oneida Lake, New York: Estimates of spatial and temporal manganese flux. Can. J. Fish. Aquat. Sci. **51:** 185–196.

ALLER, R. C. 1994. The sedimentary Mn cycle in Long Island Sound: Its role as intermediate oxidant and influence of bioturbation. J. Mar. Res. **52:** 259–295.

———, AND OTHERS. 1991. Biogeochemical processes in Amazon shelf sediments. Oceanography **52:** 281–289.

BAK, F., AND N. PFENNIG. 1991. Microbial sulfate reduction in littoral sediment of Lake Constance. FEMS Microbiol. Ecol. **85:** 31–42.

BEETON, A. M. 1969. Changes in the environment and biota of the Great Lakes, p. 150–187. *In* Eutrophication: Causes, consequences, and correctives. National Academy of Science.

BERNER, R. A. 1980*a*. A rate model for organic matter decomposition during bacterial sulfate reduction in marine sediments. Colloq. Int. Cent. Natl. Rech. Sci. **293:** 35–44.

———. 1980*b*. Early diagenesis, a theoretical approach. Princeton Univ. Press.

———, AND J. T. WESTRICH. 1985. Bioturbation and the early diagenesis of carbon and sulfur. Am. J. Sci. **285:** 193–206.

BOUDREAU, B. P. 1994. Is burial velocity a master parameter for bioturbation. Geochim. Cosmochim. Acta **58:** 1243–1249.

———. 1997. Diagenetic models and their implementation, 1st ed. Springer-Verlag.

BOWER, C. E., AND T. HOLM-HANSEN. 1980. A salicylate-hypochlorite method for determining ammonia in seawater. Can. J. Fish. Aquat. Sci. **37:** 794–798.

BROOKS, A. S., AND D. N. EDGINGTON. 1994. Biogeochemical control of phosphorus cycling and primary production in Lake Michigan. Limnol. Oceanogr. **39:** 961–968.

CANFIELD, D. E. 1994. Factors influencing organic carbon preservation in marine sediments. Chem. Geol. **114:** 315–329.

———, AND OTHERS. 1993*a*. Pathways of organic carbon oxidation in three continental margin sediments. Mar. Geol. **113:** 27–40.

———, B. THAMDRUP, AND J. W. HANSEN 1993*b*. The anaerobic degradation of organic matter in Danish coastal sediments: Iron reduction, manganese reduction, and sulfate reduction. Geochim. Cosmochim. Acta **57:** 3867–3883.

CAPONE, D. G., AND R. P. KIENE. 1988. Comparisons of microbial dynamics in marine and freshwater sediments: Contrasts in anaerobic carbon catabolism. Limnol. Oceanogr. **33:** 725–749.

CHIDTHAISONG, A., AND R. CONRAD. 2000. Turnover of glucose and acetate coupled to reduction of nitrate, ferric iron and sulfate and to methanogenesis in anoxic rice field soil. FEMS Microbiol. Ecol. **31:** 73–86.

CHRISTENSEN, E. R., AND P. K. BHUNIA. 1986. Modeling radiotracers in sediments: Comparison with observations in Lakes Huron and Michigan. J. Geophys. Res. **91:** 8559–8571.

CLINE, D. 1969. Spectrophotometric determination of hydrogen sulfide in natural waters. Limnol. Oceanogr. **14:** 454–548.

DEVOL, A. H., AND J. P. CHRISTENSEN. 1993. Benthic fluxes and nitrogen cycling in sediments of the continental margin of the eastern North Pacific. J. Mar. Res. **51:** 345–372.

EADIE, B. J., R. CHAMBERS, W. GARDNER, AND G. BELL. 1984. Sediment trap studies in Lake Michigan: Resuspension and chemical fluxes in the southern basin. J. Great Lakes Res. **10:** 307–321.

FAHNENSTIEL, G. L., AND D. SCAVIA. 1987. Dynamics of Lake Michigan phytoplankton: Recent changes in surface and deep communities. Can. J. Fish. Aquat. Sci. **44:** 509–514.

FITZGERALD, S. A. 1989. The biochemistry of amino acids in sediments from the Great Lakes. Ph.D. dissertation, Univ. of Wisconsin.

FOSSING, H., AND B. B. JØRGENSEN. 1989. Measurement of bacterial sulfate reduction in sediments: Evaluation of a single-step chromium reduction method. Biogeochemistry **8:** 223–245.

FROELICH, P. N., AND OTHERS. 1979. Early oxidation of organic matter in pelagic sediments of the eastern equatorial Atlantic: Suboxic diagenesis. Geochim. Cosmochim. Acta **43:** 1075–1090.

GRANT, J., C. W. EMERSON, B. T. HARGRAVE, AND J. L. SHORTLE. 1991. Benthic oxygen consumption on continental shelves off Eastern Canada. Cont. Shelf Res. **11:** 1083–1097.

GRASSHOFF, K., M. ERHARDT, AND K. KREMLING. 1983. Methods of seawater analysis, 2nd ed. Verlag Chemie.

HALL, P. O. J., AND R. C. ALLER. 1992. Rapid, small-volume, flow injection analysis for TCO_2 and NH_4^+ in marine and freshwaters. Limnol. Oceanogr. **37:** 1113–1119.

HANSEN, J. W., B. THAMDRUP, AND B. B. JØRGENSEN. 2000. Anoxic incubation of sediment in gas-tight plastic bags: A method for biogeochemical process studies. Mar. Ecol. Prog. Ser. **208:** 273–282.

HERMANSON, M., AND E. R. CHRISTENSEN. 1991. Recent sedimentation in Lake Michigan. J. Great Lakes Res. **17:** 33–50.

HOLMER, M., AND P. STORKHOLM. 2001. Sulphate reduction and sulphur cycling in lake sediments: A review. Freshw. Biol. **46:** 431–451.

INGVORSEN, K., AND T. D. BROCK. 1982. Electron flow via sulfate reduction and methanogenesis in the anaerobic hypolimnon of Lake Mendota. Limnol. Oceanogr. **27:** 559–564.

———, AND B. B. JØRGENSEN. 1984. Kinetics of sulfate uptake by freshwater and marine species of *Desulfovibrio.* Arch. Microbiol. **139:** 61–66.

JENSEN, M. M., B. THAMDRUP, S. RYSGAARD, M. HOLMER, AND H. FOSSING. 2003. Rates and regulation of microbial iron reduction in sediments of the Baltic-North Sea transition. Biogeochemistry **65:** 295–317.

JØRGENSEN, B. B. 1978. A comparison of methods for the quantification of bacterial sulfate reduction in coastal marine sediments. I. Measurement with radiotracer techniques. Geomicrobiol. J. **1:** 11–27.

KAPPLER, A., M. BENZ, B. SCHINK, AND A. BRUNE. 2004. Electron shuttling via humic acids in microbial Fe(III) reduction in a freshwater sediment. FEMS Microbiol. Ecol. **47:** 85–92.

KELLY, C. A., AND J. W. M. RUDD. 1984. Epilimnetic sulfate reduction and its relationship to lake acidification. Biogeochemistry **1:** 63–78.

KOSTKA, J. E., B. GRIBSHOLT, E. PETRIE, D. DALTON, H. SKELTON, AND E. KRISTENSEN. 2002. The rates and pathways of carbon oxidation in bioturbated saltmarsh sediments. Limnol. Oceanogr. **47:** 230–240.

———, E. HAEFELE, R. VIEHWEGER, AND J. W. STUCKI. 1999. Respiration and dissolution of iron (III)–containing clay minerals by bacteria. Environ. Sci. Technol. **33:** 3127–3133.

———, AND G. W. I. LUTHER. 1994. Partitioning and speciation of solid phase iron in saltmarsh sediments. Geochim. Cosmochim. Acta **58:** 1701–1710.

KRISTENSEN, E., AND F. Ø. ANDERSEN. 1987. Determination of organic carbon in marine sediments: A comparison of two CHN-analyzer methods. J. Exp. Mar. Biol. Ecol. **109:** 15–23.

KUIVILA, K. M., J. W. MURRAY, A. H. DEVOL, AND P. C. NOVELLI. 1989. Methane production, sulfate reduction and competition for substrates in the sediments of Lake Washington. Geochim. Cosmochim. Acta **53:** 409–416.

LORD, C., III. The chemistry and cycling of iron, manganese, and sulfur in salt marsh sediments. 1980. Ph.D. dissertation, Univ. of Delaware, Newark.

LOVLEY, D. R., AND M. J. KLUG. 1986. Model for the distribution of sulfate reduction and methanogenesis in freshwater sediments. Geochim. Cosmochim. Acta **50:** 11–18.

———, AND E. J. P. PHILLIPS. 1987. Competitive mechanisms for inhibition of sulfate reduction and methane production in the zone of ferric iron reduction in sediments. Appl. Environ. Microbiol. **53:** 2636–2641.

———, AND ———. 1988. Novel mode of microbial energy metabolism: organic carbon oxidation coupled to dissimilatory reduction of iron or manganese. Appl. Environ. Microbiol. **54:** 1472–1480.

MACGREGOR, B. J., D. P. MOSER, B. J. BAKER, E. W. ALM, M. MAURER, K. H. NEALSON, AND D. A. STAHL. 2001. Seasonal and spatial variability in Lake Michigan sediment small-subunit rRNA concentrations. Appl. Environ. Microbiol. **67:** 3908–3922.

MACKIN, J. E., AND R. C. ALLER. 1984. Ammonium adsorption in marine sediments. Limnol. Oceanogr. **29:** 250–257.

———, R. M. OWEN, AND P. A. MEYERS. 1980. A factor analysis of elemental associations in the surface microlayer of Lake Michigan and its fluvial inputs. J. Geophys. Res. **85:** 1563–1569.

MADENJIAN, C. P., AND OTHERS. 2002. Dynamics of the Lake Michigan food web, 1970–2000. Can. J. Fish. Aquat. Sci. **59:** 736–753.

MCKEE, J. D., T. P. WILSON, AND D. T. LONG. 1989. Pore water profiles and early diagenesis of Mn, Cu, and Pb in sediments from large lakes. J. Great Lakes Res. **15:** 68–83.

MEYERS, P. A., AND B. J. EADIE. 1993. Sources, degradation and recycling of organic matter associated with particles in Lake Michigan. Org. Geochem. **20:** 47–56.

———, S. J. EDWARDS, AND B. J. EADIE. 1980. Fatty acid and hydrocarbon content of settling sediments in Lake Michigan. J. Great Lakes Res. **6:** 331–337.

MITCHELL, M. J., S. C. SCHINDLER, J. S. OWEN, AND S. A. NORTON. 1988. Comparison of sulfur concentrations within lake sediment profiles. Hydrobiology **157:** 219–229.

MULSOW, S., B. P. BOUDREAU, AND J. N. SMITH. 1998. Bioturbation and porosity gradients. Limnol. Oceanogr. **43:** 1–9.

NALEPA, T. F., D. J. HARTSON, D. L. FANSLOW, G. A. LANG, AND S. J. LOZANO. 1998. Declines in benthic macroinvertebrate populations in southern Lake Michigan, 1980–1993. Can. J. Fish. Aquat. Sci. **55:** 2402–2413.

———, ———, J. BUCHANAN, J. F. CAVALETTO, G. A. LANG, AND S. J. LOZANO. 2000. Spatial variation in density, mean size and physiological condition of the holarctic amphipod *Diporeia* spp. in Lake Michigan. Freshw. Biol. **43:** 107–119.

POSTMA, D., AND C. A. J. APPELO. 2000. Reduction of Mn-oxides by ferrous iron in a flow system: Column experiment and reactive transport modeling. Geochim. Cosmochim. Acta **64:** 1237–1247.

RODEN, E. E., AND J. W. EDMONDS. 1997. Phosphate mobilization in iron-rich anaerobic sediments: Microbial Fe(III) oxide reduction versus iron-sulfide formation. Arch. Hydrobiol. **139:** 347–378.

———, AND J. H. TUTTLE. 1993. Inorganic sulfur turnover in oligohaline estuarine sediments. Biogeochemistry **22:** 81–105.

———, AND R. G. WETZEL. 1996. Organic carbon oxidation and suppression of methane production by microbial Fe(III) oxide reduction in vegetated and unvegetated freshwater wetland sediments. Limnol. Oceanogr. **41:** 1733–1748.

———, AND ———. 2002. Kinetics of microbial Fe(III) oxide reduction in freshwater wetland sediments. Limnol. Oceanogr. **47:** 198–211.

SCHIPPERS, A., AND B. B. JØRGENSEN. 2001. Oxidation of pyrite and iron sulfide by manganese dioxide in marine sediments. Geochim. Cosmochim. Acta **65:** 915–922.

STOOKEY, L. L. 1970. Ferrozine—a new spectrophotometric reagent for iron. Anal. Chem. **42:** 779–782.

SØRENSEN, J. 1982. Reduction of ferric iron in anaerobic, marine sediment and interaction with reduction of nitrate and sulfate. Appl. Environ. Microbiol. **43:** 319–324.

THAMDRUP, B. 2000. Bacterial manganese and iron reduction in aquatic sediments. Adv. Microb. Ecol. **16:** 41–82.

———, AND D. E. CANFIELD. 1996. Pathways of carbon oxidation in continental margin sediments off central Chile. Limnol. Oceanogr. **41:** 1629–1650.

———, H. FOSSING, AND B. B. JØRGENSEN. 1994. Manganese, iron, and sulfur cycling in a coastal marine sediment (Aarhus Bay, Denmark). Geochim. Cosmochim. Acta **58:** 5115–5129.

URBAN, N. R., P. L. BREZONIK, L. A. BAKER, AND L. A. SHERMAN. 1994. Sulfate reduction and diffusion in sediments of little-rock lake, Wisconsin. Limnol. Oceanogr. **39:** 797–815.

———, C. DINKEL, AND B. WEHRLI. 1997. Solute transfer across the sediment surface of a eutrophic lake. I. Porewater profiles from dialysis samplers. Aquat. Sci. **59:** 1–25.

VAN RAAPHORST, W., AND J. F. P. MALSCHAERT. 1996. Ammonium adsorption in superficial North Sea sediments. Cont. Shelf Res. **16:** 1415–1435.

WESTRICH, J. T., AND R. A. BERNER. 1984. The role of sedimentary organic matter in bacterial sulfate reduction: The G model tested. Limnol. Oceanogr. **29:** 236–249.

WOLLAST, R. 1991. The coastal organic carbon cycle: Fluxes, sources, and sinks, p. 365–381. *In* R. Mantoura, J.-M. Martin, and R. Wollast [eds.], Ocean marine processes global change. Wiley.

Received: 26 January 2004
Accepted: 31 May 2004
Amended: 22 June 2004